Materials Today Communications 1 (2014) 34–41

Contents lists available at ScienceDirect

Materials Today Communications

journal homepage: www.elsevier.com/locate/mtcomm

Free radical induced graft copolymerization of ethyl acrylate onto SOY for multifunctional materials

Vijay Kumar Thakur, Michael R. Kessler*

School of Mechanical and Materials Engineering, Washington State University, WA, USA

ARTICLE INFO

Article history:
Received 11 September 2014
Accepted 12 September 2014
Available online 28 September 2014

Keywords:
Soy
Graft copolymerization
Polymers
Multifunctional materials
Composites

ABSTRACT

Soy flour, here referred as SOY, is a low-cost, environmentally friendly, biodegradable, and biorenewable material available in excess amount in the United States. However, its hydrophilic nature limits the use of SOY in many commercial applications. The present research attempts to alter the surface characteristics of SOY via free radical induced graft copolymerization with ethyl acrylate. Different reaction conditions were investigated in order to achieve an optimum degree of grafting of ethyl acrylate monomer onto the SOY. The synthesized graft copolymers were characterized by different techniques to determine the interaction mechanisms between reaction monomer and SOY. Polymer composites were subsequently fabricated to assess the potential of modified SOY for different applications. Composites reinforced by graft polymerized SOY exhibited significantly increased storage modulus.

1. Introduction

Last few years have seen a tremendous interest in polymer based materials from both scientific and industrial perspectives as a result of the increasing economic impact of polymers [1–5]. Polymer based materials have affected everyday' s life in many domains directly/indirectly [6–11]. A number of biorenewable polymers, especially natural polysaccharides, have been extensively researched because of their low cost, ready availability and biodegradability [12–18]. Although both natural and synthetic polymers offer a number of advantages compared to ceramic and metallic materials, they are not well-suited for certain applications [19,20]. One way to obtain the new polymeric materials with tailored properties is the hybridization of existing materials [5]. Generally, the properties of polymers are modified either by the addition of fillers and various reinforcements, some of which result in the formation of micro/nano composites [1] or through surface functionalization [21–23]. Biorenewable polymers have seen a resurgence in a number of applications triggered by rising environmental and energy concerns [24–26]. In order to make our environment green and human friendly, interest in replacing synthetic polymers with renewable resources for new applications is increasing unceasingly [11,27,28].

Among various biobased materials recently being used in a number of applications, soy based materials such as soy protein, soy concentrate and soy flour have been the subject of frequent research [5,29]. Soy beans are an annual crop abundantly available all around the globe [30]. Their ready availability, biodegradability, renewable character, functional properties, environmental friendliness, low cost, no health risk, ability to provide unique properties through structural modification open a wide range of applications for soy [11,31]. Soy-based proteins and other derivatives, such as soy concentrate, had already demonstrated their effectiveness for a number of applications ranging from food to automotive industry [32]. Soy flour is of enormous importance among soy based materials, for application in green composites. Soy flour has been found to be available in abundant amounts in the United States as a by-product of the soybean industry [33]. Soy flour is often referred as SOY and is the cheapest among the soybean derivatives and is considered as waste materials [31]. Recently, the potential of soy flour as an indispensable component in polymer matrices as reinforcement have been explored. Soy flour is the combination of soy protein and its associated carbohydrates. It has been reported to generally contain approximately 56% protein, and the balance is carbohydrates and fats. In spite of several advantages, the hydrophilic nature of soy flour limits its applications in composite field due to the incompatibility between the hydrophilic reinforcement and hydrophobic polymer matrix. So to overcome these disadvantages, in the present work graft copolymerization of soy flour was carried out. A significant amount of literature has been reported on the graft copolymerization of vinyl monomers

* Corresponding author. Tel.: +1 509 335 8654; fax: +1 509 335 4662.
E-mail address: MichaelR.Kessler@wsu.edu (M.R. Kessler).

http://dx.doi.org/10.1016/j.mtcomm.2014.09.003
2352-4928/

onto natural polymers including soy proteins [34–36]. However a limited information is available on the graft copolymerization of ethyl acrylate monomer onto Soy flour for polymer composite applications [27,28]. The objective of the present investigation was to provide detailed information on the effect of ethyl acrylate graft copolymerization onto soy flour for diverse applications. The results were correlated with the different properties and compatibility of the grafted soy flour with the polymer matrices used to prepare the composites. Polymer composites were prepared with both the grafted and un-grafted SOY as reinforcement and poly (methyl methacrylate) (PMMA) as the matrix. Subsequently (SOY/EA-g-SOY)/PMMA composite films were prepared by compression molding.

2. Experimental

2.1. Materials

Soy flour (SOY) was provided by ADM Specialty Products-Oilseeds, Decatur, IL, USA. Ethyl acrylate (EA) monomer, a radical initiator (ammonium persulphate), and poly (methyl methacrylate) were purchased from Sigma–Aldrich. Ascorbic acid was purchased from Fisher Chemical Ltd. All chemicals were used as received without any additional purification.

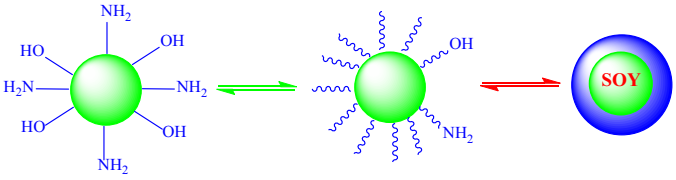

Scheme 1. Structural representation of SOY.

2.2. Synthesis of ethyl acrylate grafted SOY copolymers (EA-g-SOY)

A solution with a pH between 10 and 12 was prepared in a reaction flask by the addition of sodium hydroxide to a known amount of water. Subsequently, 2 g SOY was charged into the flask and mixed at high speed for 60 min at 95 °C. Then, a specific amount of sodium metabisulfite was added to the flask for 2 h at 85 °C to cleave the disulfide bonds of SOY. The temperature of the reaction flask was adjusted to 75 °C and catalytic amounts of the ammonium persulphate/ascorbic acid (as redox initiator) and ethyl acrylate (as

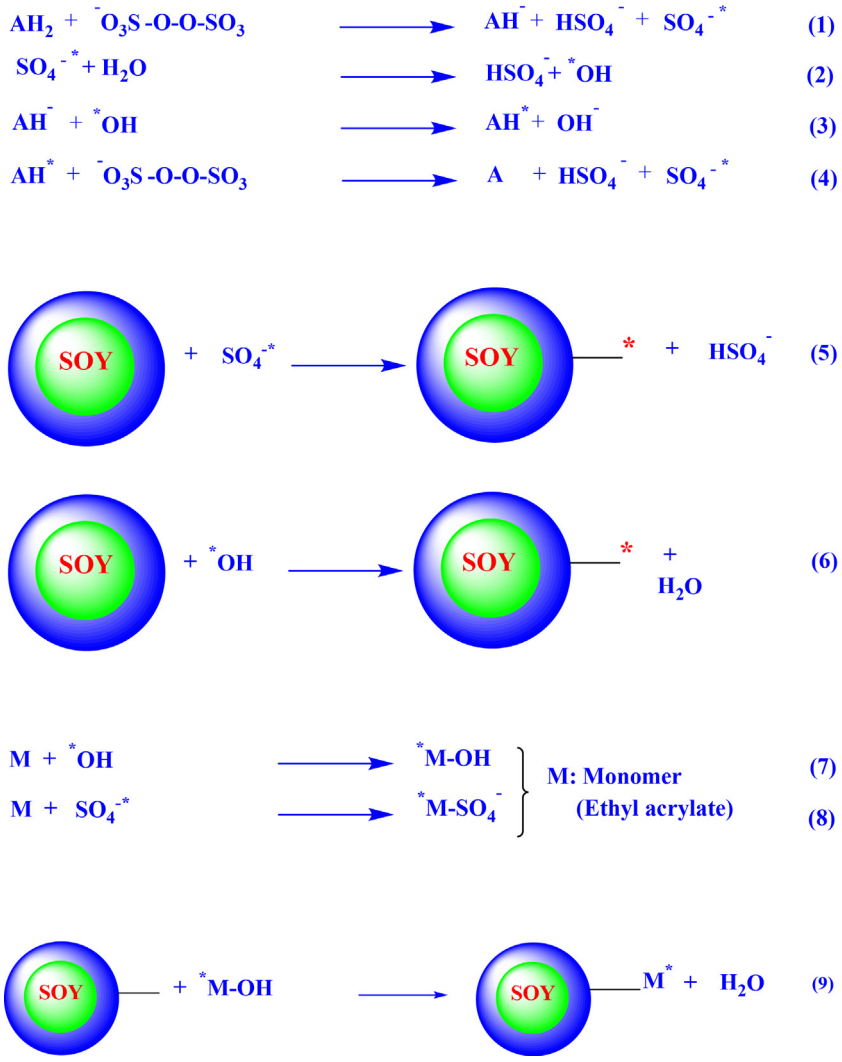

Scheme 2. Graft copolymerization mechanism of ethyl acrylate and SOY.

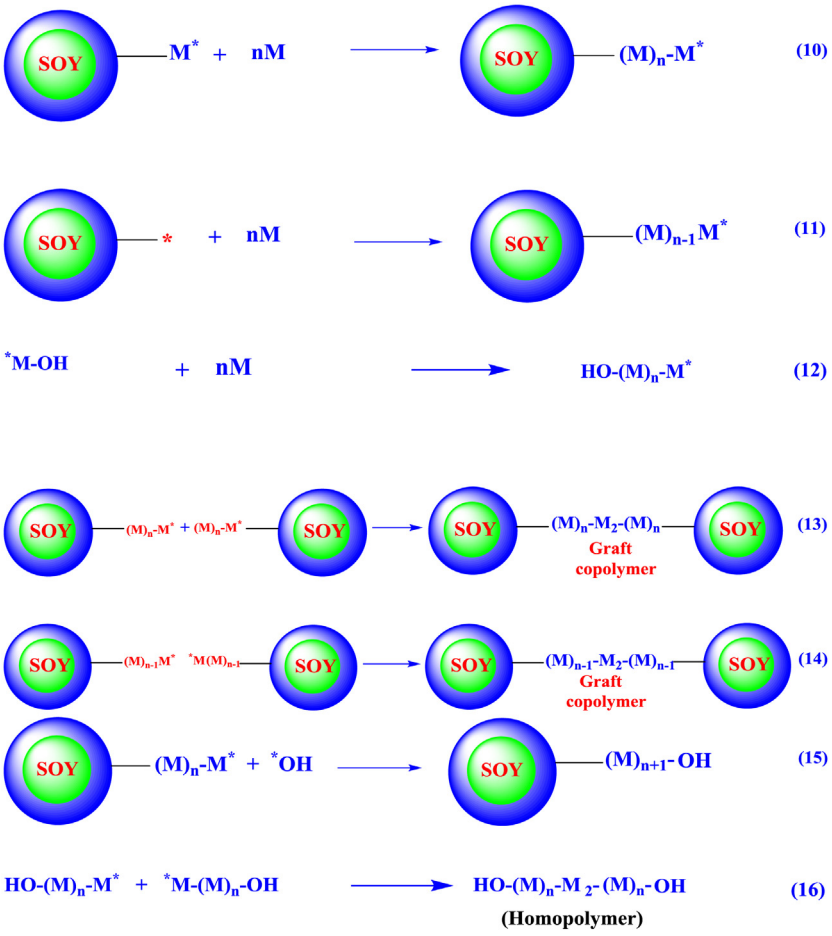

Scheme 2 (*Continued*).

monomer) were added for the synthesis of EA-g-SOY. The resulting solution was stirred at high speed and allowed to react at 50 °C for 3 h. After completion of the graft copolymerization reaction, the rudimentary product was extracted with acetone for 72 h to remove the homopolymer formed during the reaction as well as any unreacted monomer. The EA-g-SOY graft copolymer was then first dried at 50 °C for 24 h, and subsequently at 70 °C for 48 h to remove water. Subsequently the degree of grafting was calculated using the following equation:

$$P_g = \frac{W_g - W}{W} \times 100 \quad (1)$$

where W weight of pristine SOY; W_g weight of EA grafted SOY.

2.3. Preparation of (SOY/EA-g-SOY)/PMMA composite films

Pristine SOY and EA-g-SOY samples were dried in a hot air oven at 70 °C for 20 h to ensure the removal of any residual moisture in the samples. Subsequently, PMMA was melt mixed with pristine SOY and copolymerized EA-g-SOY at 5 weight % loadings at 200 °C using a twin screw microcompounder from DACA Instruments, CA, USA. The residence time for the (SOY/EA-g-SOY)/PMMA melt in the barrel was maintained at 5 min to homogenize the melt. Subsequently the extruded samples were pelletized and compression molded at 210 °C to prepare film samples with dimensions of 50 mm × 50 mm × 1 mm using a compression molding machine from Wabash MPI, IN, USA.

2.4. Characterization of PMMA/EA-g-SOY copolymer films

Fourier-transform infrared spectroscopy (FTIR) was used to identify the functional groups present in pristine SOY and EA-g-SOY. The thermal stability of pristine SOY and EA-g-SOY samples was determined by thermogravimetric analysis (TGA) using a TGA-Q50 from TA Instruments (New Castle, DE, USA) in nitrogen atmosphere at a heating rate of 20 °C/min. The dynamic mechanical behavior of pristine PMMA, SOY/PMMA composites, and EA-g-SOY/PMMA composites was characterized using a dynamic mechanical analyzer (DMA model Q800) from TA instruments (New Castle, DE, USA) in tensile mode. Temperature sweep tests were carried out between 30 and 200 °C at a frequency of 1 Hz, with a strain amplitude of 0.05% and at a heating rate of 3 °C/min. The storage modulus (E') and damping coefficient tan δ were measured as functions of temperature. The morphology of the surfaces of the SOY/EA-g-SOY copolymers was studied using scanning electron microscopy (SEM, SUPRA35, Zeiss, Germany).

3. Results and discussion

A wide variety of soy based materials have been used in the polymer composites applications either as the polymer matrix material or the reinforcement. Among these soy flour is of utmost importance from the economical point of view. Soy flour has been found to generally contain approx. 56% protein and carbohydrates. Scheme 1 depicts the structural representation of soy flour. The presence of hydroxyl and amino functional groups (—NH_2 and OH) makes soy flour suitable for modification through graft copolymerization as

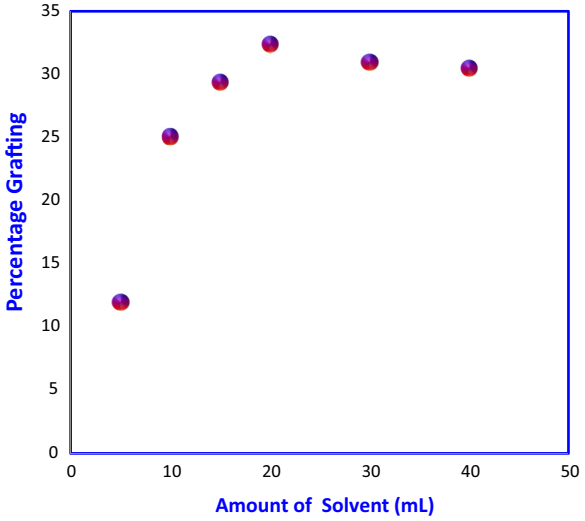

Fig. 1. Effect of solvent (water) on percentage of graft copolymerization.

these functional group are susceptible to breakage by the chemical initiator used in the synthesis. During graft copolymerization synthesis reaction, the initiator creates the necessary reactive sites on the functional groups of soy flour. The graft copolymerization reaction of ethyl acrylate onto SOY is completed in three steps: chain initiation, propagation, and termination. Eqs. (1)–(16) in Scheme 2 show the detailed mechanisms of graft copolymerization of ethyl acrylate monomer onto the SOY backbone. Eqs. (1)–(4) depicts the formation of free radical in the synthesis reaction and these free radicals are subsequently involved in the chain initiation, chain propagation and chain termination reactions (Eqs. (5)–(16)).

These mechanisms are based on the same principles as of those reported in the literature for natural biopolymers [17,18]. In order to achieve the optimum degree of grafting, different reaction parameters, such as solvent amount, reaction time, temperature, initiator, and monomer concentration were optimized. The results are discussed in detail in the following section.

3.1. *Effect of solvent*

The degree of grafting of ethyl acrylate onto SOY was studied as a function of the amount of solvent (water). Fig. 1 shows that the degree of grafting increased steadily with an increase in the

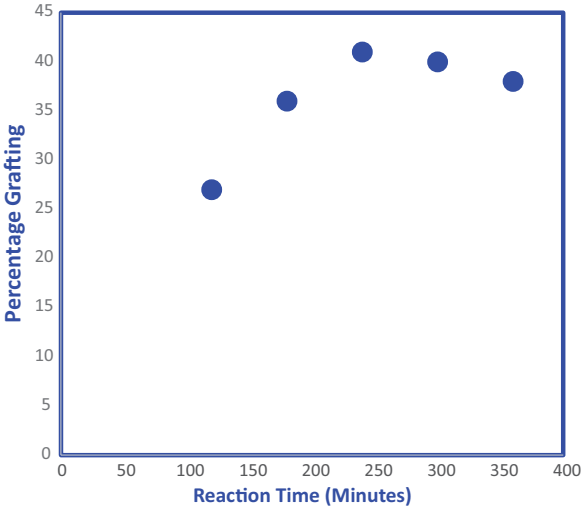

Fig. 2. Effect of reaction time on percentage of graft copolymerization.

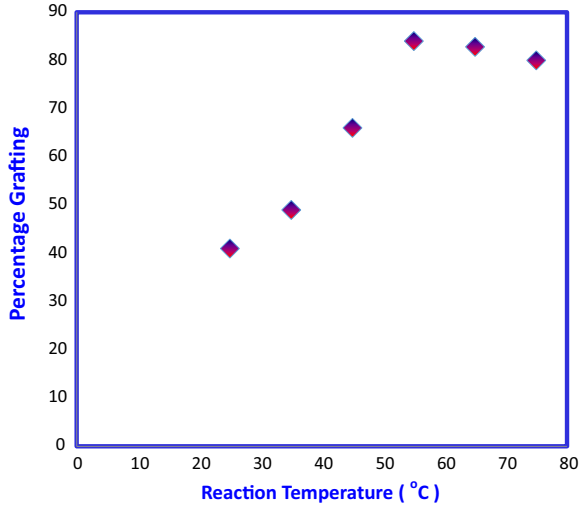

Fig. 3. Effect of reaction temperature on percentage of graft copolymerization.

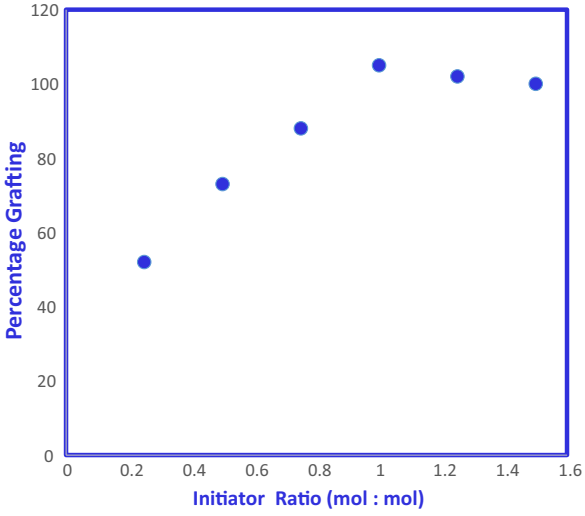

Fig. 4. Effect of initiator ratio on percentage of graft copolymerization.

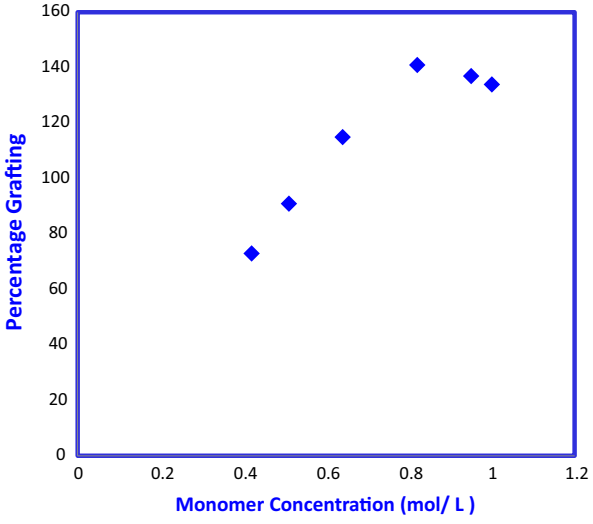

Fig. 5. Effect of monomer concentration on percentage of graft copolymerization.

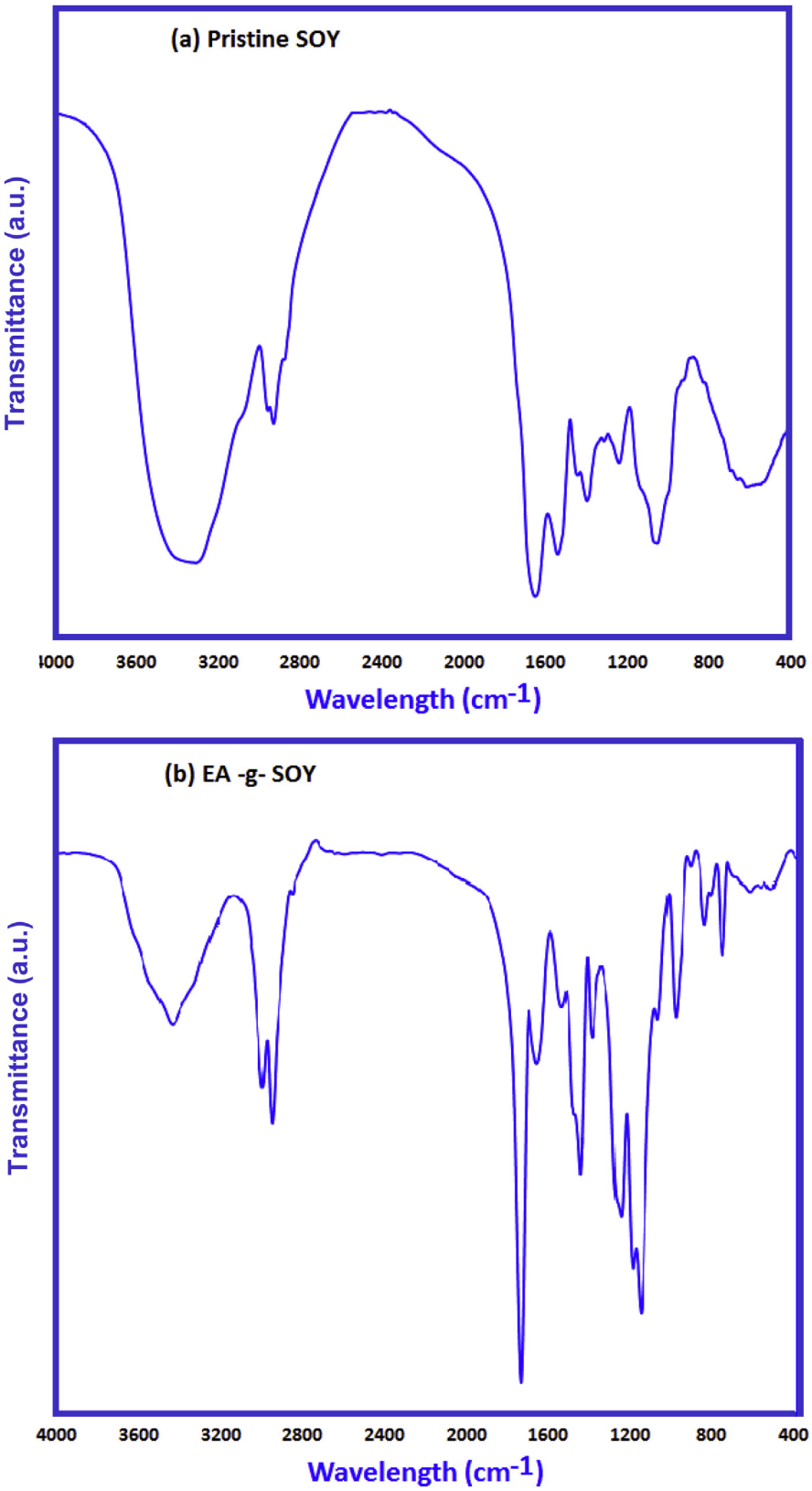

Fig. 6. FTIR spectrum of (a) pristine SOY and (b) EA-g-SOY.

amount of water up to 20 mL. A further increase in the amount of solvent resulted in a decrease in the degree of grafting, which was attributed to the fact that higher amounts of water may have inhibited the interaction between the two reaction components (SOY and the growing graft chains) leading to a lower degree of grafting.

3.2. *Effect of reaction time*

The degree of grafting of ethyl acrylate onto SOY was studied as a function of reaction time and the results are presented in Fig. 2. The degree of grafting initially increased with an increase in

reaction time and then decreases. Although the effect of time is not much significant on percentage grafting. The percentage grafting was found to increase up to 4 h beyond which it decreases due to the abridged availability of radical sites on the SOY back bone. The abridged availability of the radical sites has been attributed to the abstraction process.

3.3. Effect of reaction temperature

Graft copolymerization of ethyl acrylate and SOY was carried out at different temperatures, ranging from 25 to 75 °C and Fig. 3 shows the effect of reaction temperature on graft copolymerization. The degree of grafting increased with increasing temperature up to 55 °C while it decreased at higher temperatures. The decrease in the degree of grafting was attributed to homo-polymerization at higher temperatures as the reaction was accelerated with the increasing level of kinetic energy. In addition, disintegration of the graft copolymers may have occurred at higher temperatures.

3.4. Effect of initiator concentration

Fig. 4 depicts the effect of initiator ratio ascorbic acid:ammonium persulphate (AAc:APS) on the degree of grafting, which increased with increasing initiator ratio up to (1:1), beyond which it decreased. The initial increase in percentage grafting was attributed to the formation of a large number of free radicals in the reaction system, which facilitated the graft copolymerization synthesis reaction. However, one an optimal ratio was reached, the free radicals that initiate grafting were saturated and extra free radicals initiated homo-polymerization of ethyl acrylate, causing a decrease in the degree of grafting.

3.5. Effect of monomer concentration

The effect of the concentration of ethyl acrylate (EA) monomer on to the degree of grafting was studied for monomer amounts from 0 to 1 mol/L. Fig. 5 depicts the degree of grafting of ethyl acrylate onto SOY, which increased with increasing monomer (EA) levels up to 0.82 mol/L. With higher levels of monomer the degree of grafting started to decrease slowly. This effect was attributed to the fact that most of the reactive sites were reacted at 0.82 mol/L of monomer and there were no sites available for further reaction with the SOY backbone. Thus, once the optimum concentration of monomer was reached, the monomer molecules reacted with each other, leading to EA homo-polymerization and ultimately decreasing the degree of grafting. From the above results it is clear that the reaction parameters namely amount of solvent, reaction time, reaction temperature, initiator and monomer concentrations affect the percentage of grafting. These reaction parameters determine the relative population of the different radical species formed during different reaction steps in the graft copolymerization reaction and play an imperative role in determining overall percentage of grafting.

3.6. Chemical characterization of pristine SOY and EA-g-SOY copolymer

Fig. 6a and b shows the FTIR spectra of pristine SOY and EA-g-SOY. Fig. 6a shows the broad band at 3411 cm^{-1} for SOY, which was attributed to the stretching mode of the O—H/N—H groups. The band at 1664 cm^{-1} was assigned to the C=O stretching of the amide group (amide-I). The band 1547 cm^{-1} was assigned to N—H bending (amide-II). The spectrum of EA-g-SOY exhibited new characteristics peaks in addition to the parental peaks of SOY (Fig. 6b). The EA-g-SOY copolymer displayed a carbonyl stretching band at

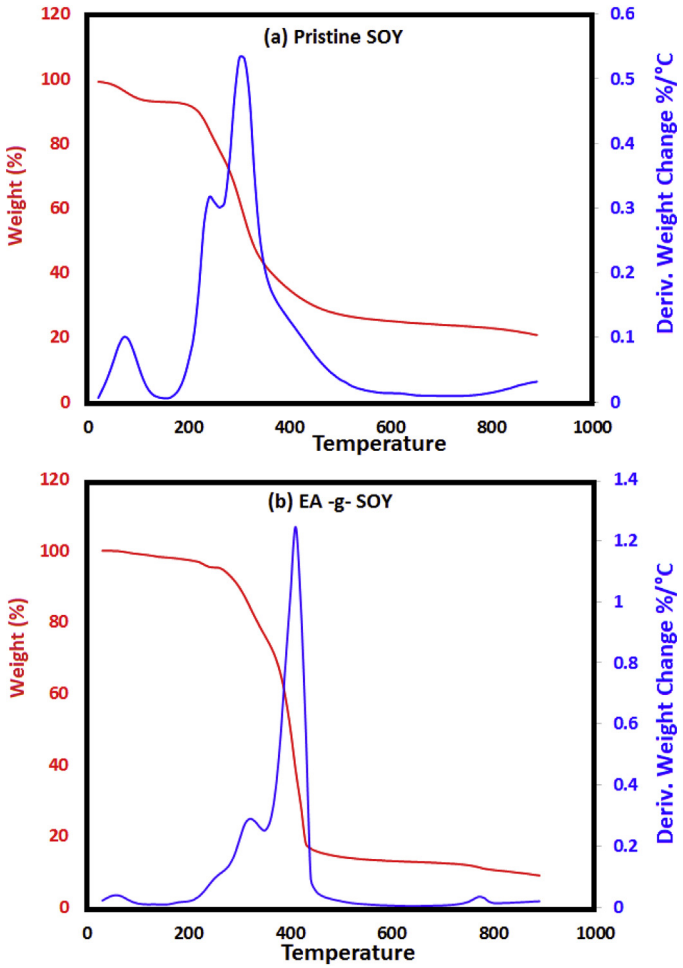

Fig. 7. TGA/DTG of (a) pristine SOY and (b) EA-g-SOY.

1735 cm^{-1} that was assigned to ethyl acrylate monomer. In addition, new bands at 1153 and 1242 cm^{-1} were also observed and were attributed to the C—O stretching of poly ethyl acrylate chains bonded to the pristine soy.

The thermal stability of pristine SOY and EA-g-SOY was investigated using thermogravimetric analysis (Fig. 7a and b) in nitrogen atmosphere as a function of % weight loss versus temperature for both materials. The TGA curves of pristine SOY exhibited three discrete zones of weight loss caused by thermal degradation. The initial weight loss occurred in the temperature range between 40 and 200 °C (Fig. 7a). This weight loss was attributed to the elimination of moisture content/water molecules and the dissociation of the quaternary structure of soy proteins and carbohydrates. The second decomposition zone between 201 and 490 °C was attributed to the cleavage of peptide bonds of the amino acid residues of the SOY, as well as the dissociation of different structural bonds in protein/carbohydrate moieties. The third and final zone of weight loss occurred between 500 and 880 °C, involving the complete decomposition of proteins and carbohydrates present in the SOY. On the other hand, EA-g-SOY exhibited two zones of thermal decomposition (Fig. 7b): one in the temperature range from 240 to 460 °C, and the other from 460 to 890 °C. The thermograms show that the thermal stability of EA-g-SOY was higher than that of pristine SOY. This increase in thermal stability was attributed to the incorporation of sufficient hydrophobic poly (ethyl acrylate) chains onto the SOY backbone, further confirming the successful synthesis of EA-g-SOY copolymers through covalent bonding. DTG analysis of pristine and grafted SOY was studied as a function of rate of weight change

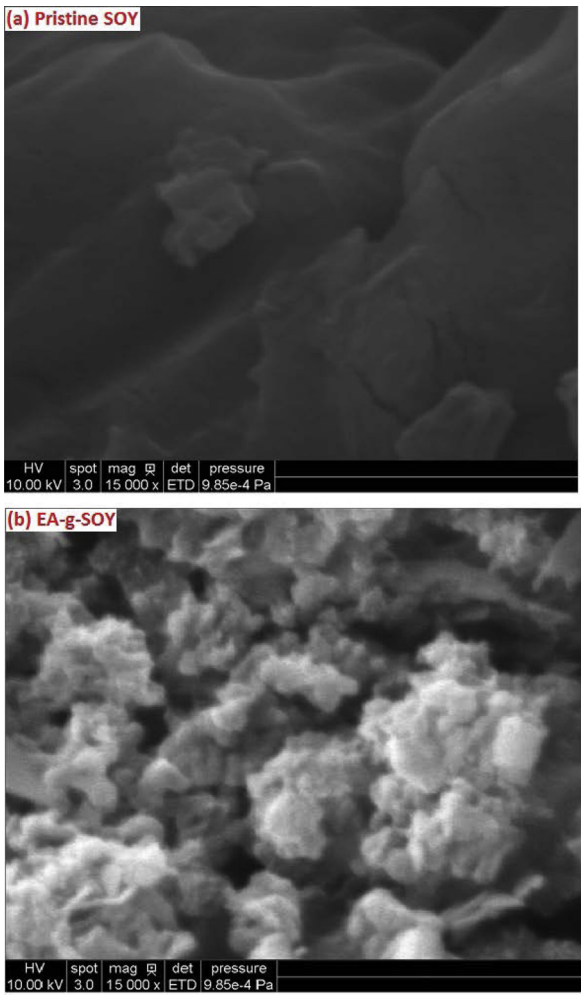

Fig. 8. Scanning electron micrograph of (a) pristine SOY and (b) EA-g-SOY.

percentage (%) versus temperature. It can be concluded from the comparative study of the thermograms that the rate of thermal decomposition was higher for SOY compared to EA-g-SOY, thus supporting the TGA results (Fig. 7a and b). The enhanced thermal stability of the EA-g-SOY copolymers was attributed to the incorporation of covalent bonding through inclusion of poly (EA) chains onto SOY back-bone (Scheme 2).

Fig. 8a and b shows the SEM images of pristine SOY and EA-g-SOY copolymers, indicating profound morphological changes in the surfaces of EA-g-SOY copolymers compared to SOY. These changes were attributed to the incorporation of ethyl acrylate chains through covalent bonding into peptide/S-S linkages and OH groups.

3.7. *Application of SOY/EA-g-SOY as reinforcement for polymer composites*

Both SOY and EA-g-SOY were investigated as potential reinforcement in polymer composites. PMMA has been used in a number of applications, ranging from electronics to automotive. It exhibits excellent properties, including hardness, high rigidity, transparency, high mechanical strength, and good insulation properties that make it a suitable matrix material for composite applications [4,27,28]. Figs. 9–11 show the dynamic mechanical analysis results for pristine PMMA, and PMMA/SOY and PMMA/EA-g-SOY composites with 5 wt.% reinforcement loadings. The DMA analyses were carried out on rectangular specimens that were

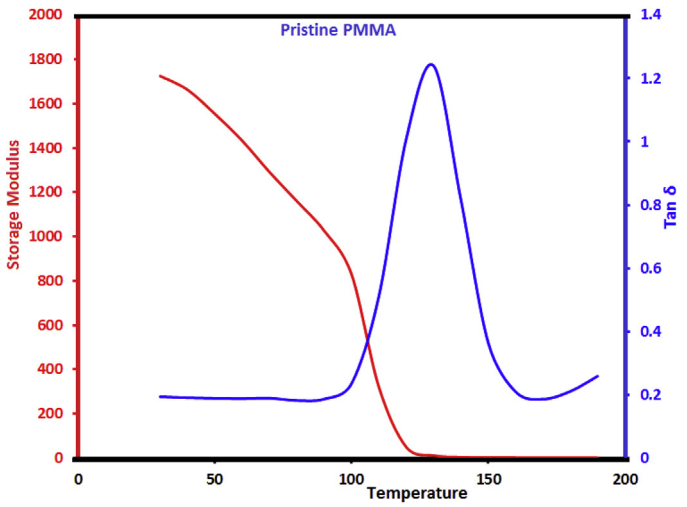

Fig. 9. Storage modulus and tan δ curves of pristine PMMA determined by dynamical–mechanical analysis.

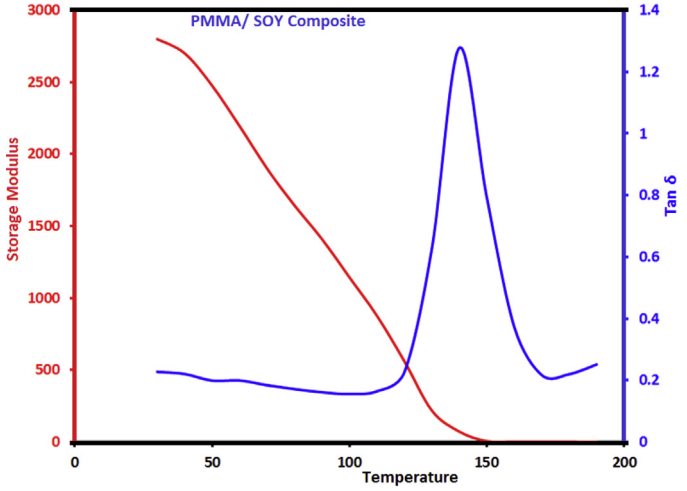

Fig. 10. Storage modulus and tan δ curves of SOY/PMMA composites determined by dynamical–mechanical analysis.

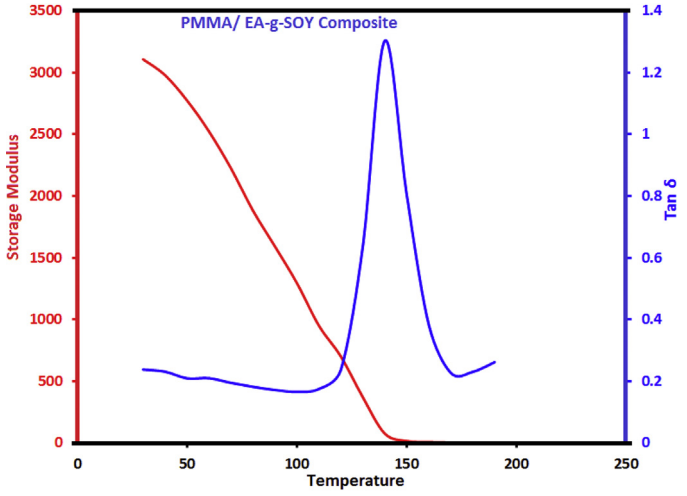

Fig. 11. Storage modulus and tan δ curves of EA-g-SOY/PMMA composites determined by dynamical–mechanical analysis.

subjected to a heating cycle at a rate of 3 °C/min and a frequency of 1 Hz. The storage modulus of PMMA increased with the incorporation of SOY and EA-g-SOY reinforcement. Figs. 10 and 11 show that the storage modulus of the PMMA/EA-g-SOY composites was higher than that of the PMMA/SOY composites, which was attributed to the better compatibility between pristine PMMA and the hydrophobic EA-g-SOY, which resulted in better load transfer at the interphase and increased stiffness [37]. In the case of pristine SOY reinforced composites, the lower storage modulus was attributed to the inhomogeneity created by the hydrophobic polymer matrix and the hydrophilic NH_2/OH group of the SOY [27,28]. The damping coefficient was also slightly higher in the composites compared to pristine PMMA. The damping coefficients ($\tan\delta = E''/E$) of the PMMA/SOY and the PMMA/EA-g-SOY composites reached a maximum as the storage modulus (E') decreased as depicted in Figs. 10 and 11. This behavior was attributed to the fact that higher temperatures provided more free movement of the polymeric chains [38].

4. Conclusion

Soy flour is an economic, viable reinforcing material for a number of applications. However, the hydrophilic nature of soy flour impedes its wide-spread application in polymer composites. In the present work, chemical induced graft copolymerization of ethyl acrylate onto soy flour was investigated to determine the effect of surface modification on the hydrophilic properties of soy flour. Soy-based graft copolymers were synthesized by optimizing different reaction conditions and characterized using FTIR, TGA, and FESEM techniques. Polymer composites were also prepared using PMMA as the matrix material. The PMMA/SOY and PMMA/EA-g-SOY composites exhibited enhanced dynamic mechanical properties compared to pristine PMMA, demonstrating the potential of SOY for use as reinforcement in composites.

Acknowledgements

This material is based upon work supported by the National Science Foundation under Grant No. CMMI1348747.

References

[1] A.I. Alateyah, H.N. Dhakal, Z.Y. Zhang, Processing, properties, and applications of polymer nanocomposites based on layer silicates: a review, Adv. Polym. Technol. (2013) 32, UNSP 21368.
[2] H.N. Dhakal, Z.Y. Zhang, N. Bennett, Influence of fibre treatment and glass fibre hybridisation on thermal degradation and surface energy characteristics of hemp/unsaturated polyester composites, Compos. B-Eng. 43 (2012) 2757–2761.
[3] V.B. Chalivendra, A. Shukla, A. Bose, V. Parameswaran, Processing and mechanical characterization of lightweight polyurethane composites, J. Mater. Sci. 38 (2003) 1631–1643.
[4] V.K. Thakur, D. Vennerberg, S.A. Madbouly, M.R. Kessler, Bio-inspired green surface functionalization of PMMA for multifunctional capacitors, RSC Adv. 4 (2014) 6677–6684.
[5] A.M. Dobos, M.-D. Onofrei, I. Stoica, N. Olaru, L. Olaru, S. Ioan, Rheological properties and microstructures of cellulose acetate phthalate/hydroxypropyl cellulose blends, Polym. Compos. 33 (2012) 2072–2083.
[6] A. Lopez-Arraiza, G. Castillo, H.N. Dhakal, R. Alberdi, High performance composite nozzle for the improvement of cooling in grinding machine tools, Compos. B-Eng. 54 (2013) 313–318.
[7] J. Crowley, V.B. Chalivendra, Mechanical characterization of ultra-high molecular weight polyethylene-hydroxyapatite nanocomposites, Biomed. Mater. Eng. 18 (2008) 149–160.
[8] M. Jawaid, H.P.S.A. Khalil, A. Abu Bakar, Mechanical performance of oil palm empty fruit bunches/jute fibres reinforced epoxy hybrid composites, Mater. Sci. Eng.-Struct. Mater. Prop. Microstruct. Process. 527 (2010) 7944–7949.
[9] D. Depan, J.S. Shah, R.D.K. Misra, Degradation mechanism and increased stability of chitosan-based hybrid scaffolds cross-linked with nanostructured carbon: process–structure–functional property relationship, Polym. Degrad. Stab. 98 (2013) 2331–2339.
[10] X. Huang, A. Netravali, Biodegradable green composites made using bamboo micro/nano-fibrils and chemically modified soy protein resin, Compos. Sci. Technol. 69 (2009) 1009–1015.
[11] A. Nesterenko, I. Alric, F. Silvestre, V. Durrieu, Comparative study of encapsulation of vitamins with native and modified soy protein, Food Hydrocoll. 38 (2014) 172–179.
[12] M. Jawaid, H.P.S.A. Khalil, A. Abu Bakar, Woven hybrid composites: tensile and flexural properties of oil palm-woven jute fibres based epoxy composites, Mater. Sci. Eng.-Struct. Mater. Prop. Microstruct. Process. 528 (2011) 5190–5195.
[13] T. Ghosh Dastidar, A.N. Netravali, Green crosslinking of native starches with malonic acid and their properties, Carbohydr. Polym. 90 (2012) 1620–1628.
[14] H.N. Dhakal, Z.Y. Zhang, R. Guthrie, J. MacMullen, N. Bennett, Development of flax/carbon fibre hybrid composites for enhanced properties, Carbohydr. Polym. 96 (2013) 1–8.
[15] S. Ioan, A.M. Necula, I. Stoica, N. Olaru, L. Olaru, Influence of casting solution characteristics on cellulose acetate membranes: rheology and atomic force microscopy, Int. J. Polym. Anal. Charact. 15 (2010) 166–181.
[16] A.M. Dobos, I. Stoica, N. Olaru, L. Olaru, E.G. Ioanid, S. Ioan, Surface properties and biocompatibility of cellulose acetates, J. Appl. Polym. Sci. 125 (2012) 2521–2528.
[17] V.K. Thakur, M.K. Thakur, R.K. Gupta, Rapid synthesis of graft copolymers from natural cellulose fibers, Carbohydr. Polym. 98 (2013) 820–828.
[18] V.K. Thakur, M.K. Thakur, R.K. Gupta, Graft copolymers of natural fibers for green composites, Carbohydr. Polym. 104 (2014) 87–93.
[19] V.K. Thakur, M.K. Thakur, Processing and characterization of natural cellulose fibers/thermoset polymer composites, Carbohydr. Polym. 109 (2014) 102–117.
[20] V.K. Thakur, M.K. Thakur, P. Raghavan, M.R. Kessler, Progress in green polymer composites from lignin for multifunctional applications: a review, ACS Sustain. Chem. Eng. 2 (2014) 1072–1092.
[21] M.A. Pinto, V.B. Chalivendra, Y.K. Kim, A.F. Lewis, Evaluation of surface treatment and fabrication methods for jute fiber/epoxy laminar composites, Polym. Compos. 35 (2014) 310–317.
[22] A.M. Necula, I. Stoica, N. Olaru, F. Doroftei, S. Ioan, Silver nanoparticles in cellulose acetate polymers: rheological and morphological properties, J. Macromol. Sci. B-Phys. 50 (2011) 639–651.
[23] V.K. Thakur, D. Vennerberg, M.R. Kessler, Green aqueous surface modification of polypropylene for novel polymer nanocomposites, ACS Appl. Mater. Interfaces 6 (2014) 9349–9356.
[24] H.N. Dhakal, Z.Y. Zhang, M.O.W. Richardson, Effect of water absorption on the mechanical properties of hemp fibre reinforced unsaturated polyester composites, Compos. Sci. Technol. 67 (2007) 1674–1683.
[25] M. Jawaid, H.P.S.A. Khalil, A. Hassan, R. Dungani, A. Hadiyane, Effect of jute fibre loading on tensile and dynamic mechanical properties of oil palm epoxy composites, Compos. B-Eng. 45 (2013) 619–624.
[26] M.A. Pinto, V.B. Chalivendra, Y.K. Kim, A.F. Lewis, Effect of surface treatment and *Z*-axis reinforcement on the interlaminar fracture of jute/epoxy laminated composites, Eng. Fract. Mech. 114 (2013) 104–114.
[27] V.K. Thakur, Kessler M.R. Synthesis, Characterization of AN-g-SOY for sustainable polymer composites, ACS Sustain. Chem. Eng. (2014), http://dx.doi.org/10.1021/sc500473a.
[28] V.K. Thakur, M. Thunga, S.A. Madbouly, M.R. Kessler, PMMA-g-SOY as a sustainable novel dielectric material, RSC Adv. 4 (2014) 18240–18249.
[29] D. Cho, A.N. Netravali, Y.L. Joo, Mechanical properties and biodegradability of electrospun soy protein Isolate/PVA hybrid nanofibers, Polym. Degrad. Stab. 97 (2012) 747–754.
[30] X. Huang, A. Netravali, Characterization of flax fiber reinforced soy protein resin based green composites modified with nano-clay particles, Compos. Sci. Technol. 67 (2007) 2005–2014.
[31] J.T. Kim, A.N. Netravali, Development of aligned-hemp yarn-reinforced green composites with soy protein resin: effect of pH on mechanical and interfacial properties, Compos. Sci. Technol. 71 (2011) 541–547.
[32] A. Nesterenko, I. Alric, F. Silvestre, V. Durrieu, Vegetable proteins in microencapsulation: a review of recent interventions and their effectiveness, Ind. Crops Prod. 42 (2013) 469–479.
[33] P. Lodha, A.N. Netravali, Thermal and mechanical properties of environment-friendly green plastics from stearic acid modified-soy protein isolate, Ind. Crops Prod. 21 (2005) 49–64.
[34] V.K. Thakur, M.K. Thakur, R.K. Gupta, Graft copolymers from cellulose: synthesis, characterization and evaluation, Carbohydr. Polym. 97 (2013) 18–25.
[35] D. Xi, C. Yang, X. Liu, M. Chen, C. Sun, Y. Xu, Graft polymerization of styrene on soy protein isolate, J. Appl. Polym. Sci. 98 (2005) 1457–1461.
[36] V.K. Thakur, M.K. Thakur, R.K. Gupta, Synthesis of lignocellulosic polymer with improved chemical resistance through free radical polymerization, Int. J. Biol. Macromol. 61 (2013) 121–126.
[37] H. Cui, M.R. Kessler, Glass fiber reinforced ROMP-based bio-renewable polymers: enhancement of the interface with silane coupling agents, Compos. Sci. Technol. 72 (2012) 1264–1272.
[38] A.L. Martínez-Hernández, C. Velasco-Santos, M. de-Icaza, V.M. Castaño, Dynamical–mechanical and thermal analysis of polymeric composites reinforced with keratin biofibers from chicken feathers, Compos. B-Eng. 38 (2007) 405–410.